Modelling nonlinear regenerative effects in metal cutting

By Gábor Stépán

Department of Applied Mechanics, Budapest University of Technology and Economics, Budapest H-1521, Hungary (stepan@mm.bme.hu)

This paper deals with the nonlinear models of regenerative chatter on machine tools. The limitations and actual problems of the existing theory are summarized. These cause difficulties in industrial applications, like in the design of optimum technological parameters, adaptive control and/or vibration-suppression strategies. An industrial machine-tool vibration case is analysed experimentally and conclusions are drawn with respect to the likely mechanism of the nonlinear behaviour in a four-dimensional phase-space representation embedded in the infinite-dimensional phase space of regenerative chatter. In some respects, the whole phenomenon seems to be analogous to the turbulence in fluid mechanics.

1. Introduction

Undesired relative vibrations between the tool and the workpiece jeopardize the quality of machined surfaces in the case of cutting. If the modal parameters (natural frequencies, proportional relative damping factors, vibration modes) are identified on a machine tool (including the actual tool and workpiece), and the cutting force is also well estimated, then there is a possibility that we may predict these vibrations, or design the technology in a way that the instability of the cutting is avoided. If these methods are fitted in technology–parameter–optimization processes and software, great financial advantage can be achieved (see Halley *et al.* 1999).

One of the most important causes of instability in the cutting process is the so-called regenerative effect. The physical basis of this phenomenon is well known in the literature. Because of some external perturbations, the tool starts a damped oscillation relative to the workpiece, and the surface of the workpiece becomes wavy. After a round of the workpiece (or tool), the chip thickness will vary at the tool because of this wavy surface. As a consequence, the cutting force depends on the actual and delayed values of the relative displacement of the tool and the workpiece, where the length of the delay is equal to the time-period τ of the revolution of the workpiece (or tool). This delay is the central idea of the regenerative effect.

There exist, of course, other physical mechanisms which lead to relative vibrations between the tool and the workpiece. One of these is related to the thermoplastic behaviour of the chip material (see Davies & Burns 1999); another important one is described via two-and-higher-degree-of-freedom vibrations in the presence of friction between the tool and chip–workpiece contact surfaces (see Grabec 1988; Wiercigroch

1997). The unification of these different kinds of models and the clarification of possible overlaps between them are still open problems.

The prediction of the regenerative vibrations is difficult in practical cases, even when the above-mentioned experimental preparatory work (modal analysis and cutting-force estimation) is carried out successfully, as shown by Minis & Berger (1998). In spite of the fact that the linear stability analysis of the stationary cutting under regenerative conditions can be considered as a solved problem on the research level, the results are rarely applied in practice and the major development efforts are taken in the direction of adaptive and/or active control of the chatter. One reason for this is the uncertainty of some of the parameters in the model. But even if the parameters are well estimated, the results of the linear stability analysis are limited. Experiments (see Hanna & Tobias 1974; Shi & Tobias 1984) in the 1970s and 1980s suggested that unstable periodic motions may exist around the otherwise stable stationary cutting, and the amplitude of this motion can be very small. In other words, the domain of attractivity of the stable cutting may be very small, and the whole cutting process may be very sensitive to perturbations. This means a serious practical limitation to the industrial applicability of the (otherwise still complicated) linear models.

The specialist literature (Stépán & Kalmár-Nagy 1997; Nayfeh *et al.* 1997; Kalmár-Nagy *et al.* 1999) of nonlinear dynamics has been dealing with this unstable periodic motion since the mid-1990s, using both analytical methods and computer simulation. The early results were often contradictory to each other and also to the experiments, and the complexity of the calculations made them inaccessible for industrial applications. In this paper, however, experimental and theoretical research results are reported which may provide simple-to-use analytical formulae on the domain of attraction of stable stationary cutting for technology design using computer algebra, and which may also help to show a deeper understanding of the nonlinear regenerative chatter. This deeper understanding is partly based on an industrial case study, where the development of quasi-periodic oscillations, chaotic ones and fractal-like machined surfaces are experienced and analysed in order to construct the topological mechanism of regenerative vibration development in a four-dimensional subspace embedded in the infinite-dimensional phase space of regenerative chatter.

2. Linear model of regenerative chatter

In order to represent the open questions related only to the time-delay effects, a cartoon model of the machine tool is first considered in the form of a one-degree-of-freedom (one-DOF) damped oscillator, with the characteristic parameters ω_n and ξ denoting the natural angular frequency of the undamped system and the relative damping factor (or dimensionless coefficient of viscous damping), respectively. This simple model can still be useful in those practical cases where there exists a well-separated lowest natural frequency and corresponding vibration mode of the machine tool (see Tlusty & Spacek 1954; Tobias 1965; Stépán 1989). The model in figure 1 shows the case of the so-called orthogonal cutting.

In spite of the fact that the single mechanical DOF gives the impression that the system can be uniquely analysed in the phase plane of the tool displacement and velocity, and so the well-known basic methods of linear and nonlinear dynamics can be used here, the corresponding mathematical model is 'infinite dimensional'; the phase space is the function space of continuous functions above the 'time' interval

Figure 1. Mechanical model of regenerative chatter for orthogonal cutting.

$[-\tau, 0]$, and nonlinear vibration phenomena may occur much more complicated than the ones expected from the mechanical DOF. In this respect, the complexity of the regenerative vibrations experienced in the cutting process can be compared with that of the turbulence phenomenon in fluid mechanics—both take place in infinite-dimensional phase spaces. This is due to the presence of the time delay τ, which is inversely proportional to the cutting speed v as explained in § 1.

The mathematical model of the above mechanical model is a delay-differential equation (DDE). The mathematical modelling of regenerative chatter goes back to the 1950s, when the theory of delay-differential equations started its development in mathematics.

Time delay often occurs in control systems, where its presence is related to the delay in the information transmission, and it is rarely experienced with a considerable value in pure mechanical systems like machine tools. Note, however, that dynamic contact problems of elasticity and/or plasticity often lead to similar delay-differential equation models, as in the case of rolling metal sheets, or when an elastic tyre rolls on a rigid ground, as shown by Stépán (1999). This similarity is not surprising when the travelling-wave-like solutions of the corresponding partial differential equation (PDE) models help to transform the two infinite-dimensional systems into each other.

In the specialist literature of control theory and mathematics it is a well-known 'rule of thumb' that increasing delay tends to destabilize any dynamical system. In other words, 'good memory causes trouble'. However, the regenerative chatter of machine tools is an exception even in this respect: in mechanical systems with low damping (like the machine-tool structures), the time delay may also have a stabilizing effect. These special cases are analysed with special attention in the mathematical literature by Kuang (1993) or Wang & Hu (1999).

Clearly, the mechanical system presented in figure 1 is linear. There have been discussions on the importance of machine-tool structure nonlinearities (see Shi & Tobias 1984; Nayfeh *et al.* 1997) relative to the cutting-force nonlinearities. It may happen that special machine-tool structure deficiencies make the corresponding structural nonlinearity important, but the detailed experimental analysis presented in the appendix of Shi & Tobias (1984) is convincing: the cutting-force nonlinearity determines most of the nonlinear vibrations.
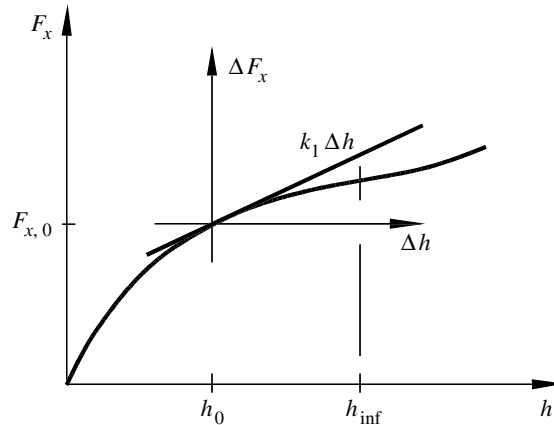
Figure 2. Nonlinear cutting-force characteristic.

The standard stationary nonlinear cutting-force dependence on chip thickness is presented in figure 2. The simplest experiment-based approximation of this function for small chip thickness ($h < 0.9h_{\text{inf}}$) is the well-known 'three-quarter rule', where the dependence on the chip width w is linear and the dependence on the cutting speed v is neglected,

$$F_x(w, h) = c_1 w h^{3/4}. \tag{2.1}$$

Its linear part at the theoretical chip thickness h_0 is described with the help of the so-called cutting coefficient k_1, defined as

$$k_1(w, h_0) = \left.\frac{\partial F_x(w, h)}{\partial h}\right|_{h_0} = \tfrac{3}{4}c_1 w h_0^{-1/4}. \tag{2.2}$$

Let $p(\theta)$ describe the shape of the stationary stress distribution along the active face of the tool in the time-domain above $\theta \in [-\sigma, 0]$, with

$$\int_{-\sigma}^{0} p(\theta)\, \mathrm{d}\theta = 1, \tag{2.3}$$

where σ is the time needed for a chip particle to slip along the active face of length l (see also figure 1). Consequently, this pressure distribution is $p(s/v)/v$ along the space coordinate $v\theta = s \in [-l, 0]$ of the tool face, where the contact length is $l = v\sigma$ and the cutting-force distribution is described by $P_x(w, h, s) = F_x(w, h)p(s/v)/v$. If this distributed force system on the tool edge can be modelled properly (for example, by experiments, simulation and special finite-element methods, as done by Usui *et al.* (1978), Davies *et al.* (1997) and Marusich & Ortiz (1995), respectively), the corresponding short time-delay effect can be integrated into the cutting-force expression, as explained by Stépán (1998). The chip-thickness variation along the active face can then be approximated as

$$\Delta h = h(t, \theta) - h_0 = x(t - \tau + \theta) - x(t + \theta), \quad t \in [t_0, \infty), \quad \theta \in [-\sigma, 0], \tag{2.4}$$

and the linear approximation of the cutting-force variation has the form

$$\Delta F_x \approx k_1 \int_{-\sigma}^{0} p(\theta)(x(t - \tau + \theta) - x(t + \theta))\, \mathrm{d}\theta. \tag{2.5}$$

When this cutting-force variation is substituted in the equation of motion of the machine-tool model, the following integro-differential equation is obtained:

$$\ddot{x} + 2\xi\omega_{\mathrm{n}}\dot{x} + \omega_{\mathrm{n}}^2 x = \frac{1}{m}\Delta F_x(\Delta h)$$

$$\Rightarrow \quad \ddot{x}(t) + 2\xi\omega_{\mathrm{n}}\dot{x}(t) + \omega_{\mathrm{n}}^2 x(t) + \frac{k_1}{m}\int_{-\sigma}^{0} p(\theta)x(t+\theta)\,\mathrm{d}\theta$$

$$-\frac{k_1}{m}\int_{-\tau-\sigma}^{-\sigma} p(\tau+\theta)x(t+\theta)\,\mathrm{d}\theta = 0. \quad (2.6)$$

In accordance with Usui *et al.* (1978), a good approximation of the shear-stress distribution can be given by an exponential function of the form

$$p(\theta) = \frac{1}{\sigma_0}\mathrm{e}^{\theta/\sigma_0}, \quad \theta \in (-\infty, 0], \quad (2.7)$$

where $\sigma_0 v = l_0$ can take the role of an approximate finite contact length, although $\sigma \to +\infty$ in this case. The mathematical advantage of this weight function is that the integrals in the equation of motion can be calculated by parts, and after differentiating the whole integro-differential equation again with respect to the time t, the following third-order DDE serves as a basic mathematical model:

$$\sigma_0 \dddot{x}(t) + (1 + 2\xi\omega_{\mathrm{n}}\sigma_0)\ddot{x}(t) + (2\xi\omega_{\mathrm{n}} + \omega_{\mathrm{n}}^2\sigma_0)\dot{x}(t)$$

$$+ \left(\omega_{\mathrm{n}}^2 + \frac{k_1}{m}\right)x(t) - \frac{k_1}{m}x(t-\tau) = 0. \quad (2.8)$$

Clearly, this model provides two well-known limit cases. When the short regenerative effect is very strong, that is, $\sigma_0 \to \infty$, then the long delay effect is negligible, and the equation of a simple damped oscillator is obtained after an integration with respect to the time t,

$$\ddot{x}(t) + 2\xi\omega_{\mathrm{n}}\dot{x}(t) + \omega_{\mathrm{n}}^2 x(t) = 0. \quad (2.9)$$

This system is always asymptotically stable, of course. When the short regenerative effect is negligible, then $\sigma_0 \to 0$, and so the pressure distribution tends to the Dirac delta function, i.e. $p(\theta) \to \delta(\theta)$, and the equation of motion assumes the form of a simple second-order delay-differential equation,

$$\ddot{x}(t) + 2\xi\omega_{\mathrm{n}}\dot{x}(t) + \left(\omega_{\mathrm{n}}^2 + \frac{k_1}{m}\right)x(t) - \frac{k_1}{m}x(t-\tau) = 0. \quad (2.10)$$

The stability of this system is well studied in the literature (see, for example, Stépán 1989), and it shows that the simplified equation of motion has serious limitations at low and high cutting speeds. The so-called dynamic cutting theory of Tobias (1965) tries to improve this simple model for low cutting speeds only, but the experimental identification of the key parameter in his model, the so-called penetration factor C, is difficult and needs special consideration for the different cases of turning, milling or drilling. Tlusty (1978) is more successful in this respect.

Note that models with more than one discrete time delay in the equations of motion also occur in the case of high-speed milling with large feed rate (together with the aforementioned time-periodic coefficients and parametric excitation), as shown by Balachandran & Zhao (2000) and Bayly *et al.* (1999) or, in the case of grinding, Davies (1998).

3. Linear stability analysis and stability charts

The stationary cutting is described by the constant chip thickness $h(t) \equiv h_0$, i.e. by the trivial solution $x(t) \equiv 0$ in the equation of motion (2.6). Its asymptotic stability in the Lyapunov sense is determined by the characteristic function D. This comes either by the application of the Laplace transformation in (2.6) or simply by the substitution of the trial solution $x(t) = A \exp(\lambda t)$, $A, \lambda \in C$,

$$D(\lambda) = \lambda^2 + 2\xi\omega_n\lambda + \omega_n^2 + \frac{k_1}{m} \int_{-\sigma}^{0} p(\theta)e^{\lambda\theta} \, d\theta - \frac{k_1}{m} \int_{-\tau-\sigma}^{-\tau} p(\tau + \theta)e^{\lambda\theta} \, d\theta. \quad (3.1)$$

When the exponential weight function (2.8) is used, this characteristic function simplifies to

$$D(\lambda) = \lambda^2 + 2\xi\omega_n\lambda + \omega_n^2 + \frac{k_1}{m}\frac{1}{1 + \sigma_0\lambda} - \frac{k_1}{m}\frac{e^{-\lambda\tau}}{1 + \sigma_0\lambda}, \quad (3.2)$$

which corresponds to the DDE (2.8) after multiplication by the denominator $1 + \sigma_0\lambda$.

The stability charts are traditionally constructed in the plane of the parameters $\Omega = 2\pi/\tau$ and k_1. The reason for this is that the cutting speed is linearly proportional to the angular velocity Ω of a cylindrical workpiece (often given in RPM), while the cutting coefficient k_1 is linearly proportional to the other important parameter, the width of cut w, as shown by (2.2).

The borders of the stability domains in the stability chart can be constructed by substituting pure imaginary characteristic roots $\lambda = i\omega$ into the characteristic function above. Then, separating its real and imaginary parts, we obtain the real functions

$$R(\omega) = \text{Re}\, D(i\omega) = -\omega^2 + \omega_n^2 + \frac{k_1}{m}\frac{1 - \cos(\omega\tau) + \sigma_0\omega\sin(\omega\tau)}{1 + \sigma_0^2\omega^2}, \quad (3.3)$$

$$S(\omega) = \text{Im}\, D(i\omega) = 2\xi\omega_n\omega + \frac{k_1}{m}\frac{\sin(\omega\tau) - \sigma_0\omega(1 - \cos(\omega\tau))}{1 + \sigma_0^2\omega^2}. \quad (3.4)$$

The $R(\omega) = 0$, $S(\omega) = 0$ equations give an infinite series of curves in the parameter plane. It is not trivial to choose the stable domains bordered by them. The mathematical theory which supports this job is given in Stépán (1989), and is based on the condition that all the infinitely many characteristic roots are located in the left half of the complex plane. The curves themselves can be expressed in a more explicit form for $\Omega = 2\pi/\tau$ and k_1, but we do not present them here because of their complexity. Still, the parameter $\omega \in ((2j - 1)\pi/\tau, 2j\pi/\tau)$, $j = 1, 2, \ldots$, appears in the formulae, which also gives the angular vibration frequency at the limit of the stability. A stability chart like this can be constructed by a simple computer program based on the above formulae, and this is presented in figure 3 for the parameters $m = 50$ kg, $\xi = 0.05$ and $\omega_n = 775$ rad s^{-1}.

As is clearly shown in figure 3, the stability limit has an almost fractal-like structure for low cutting speeds, and the shaded stable and the white unstable domains alternate for varying cutting speeds when the cutting coefficient is in the range of 3 N µm^{-1}. Also, there is an improvement in stability for low cutting speeds and for high speeds, too. The stability properties are worst in the middle range of the workpiece speed of 700 RPM. The complexity of these stability charts, even for the
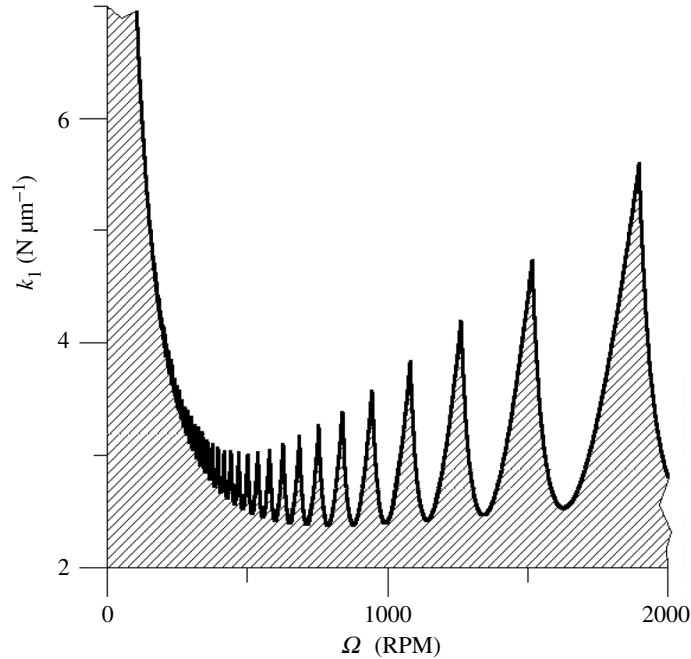
Figure 3. Stability chart with short and long regenerative effects.

simplest mechanical models like the one in figure 1, explains why it is so difficult to achieve simple-to-use practical conclusions regarding machine-tool vibrations.

When the short regenerative effect is negligible, that is, $\sigma_0 \to 0$ and the stress distribution on the active face of the tool tends to a concentrated cutting force in accordance with $p(\theta) \to \delta(\theta)$, the characteristic function (3.2) simplifies to

$$D(\lambda, k_1) = \lambda^2 + 2\xi\omega_n\lambda + \omega_n^2 + \frac{k_1}{m} - \frac{k_1}{m}e^{-\lambda\tau}, \tag{3.5}$$

and the stability limit curves in (3.3) and (3.4) become

$$-\omega^2 + \omega_n^2 + \frac{k_1}{m}(1 - \cos(\omega\tau)) = 0, \tag{3.6}$$

$$2\xi\omega_n\omega + \frac{k_1}{m}\sin(\omega\tau) = 0. \tag{3.7}$$

Now, the stability limit curves (or D curves) can be expressed easily in a relatively compact algebraic form,

$$\left.\begin{aligned}
\Omega_j(\omega) &= \frac{\pi\omega}{j\pi - \arctan[(\omega^2 - \omega_n^2)/(2\xi\omega_n\omega)]}, \quad j = 1, 2, \ldots, k_1, \\
k_1(\omega) &= \tfrac{1}{2}m\frac{(\omega^2 - \omega_n^2)^2 + 4\xi^2\omega_n^2\omega^2}{\omega^2 - \omega_n^2}.
\end{aligned}\right\} \tag{3.8}$$

Since the cutting coefficient k_1 is positive, the second formula already shows that the vibration frequency after the loss of stability will always be above the natural frequency of the system. Also, a minimum value of the cutting coefficient can be

found for some critical running speeds $\Omega_{\mathrm{cr},j}$. These are similar to the minimum values shown on the lobes of figure 3, but they are the same for each lobe. This critical minimum value of the cutting coefficient gives a conservative estimate for the stable domains and can be calculated by checking its derivative in (3.8),

$$\frac{\mathrm{d}k_1}{\mathrm{d}\omega}(\omega_{\mathrm{cr}}) = 0 \quad \Rightarrow \quad \begin{cases} \omega_{\mathrm{cr}} = \omega_{\mathrm{n}}\sqrt{1 + 2\xi}, \\ k_{1,\mathrm{min}} = 2m\omega_{\mathrm{n}}^2\xi(1 + \xi), \\ \Omega_{\mathrm{cr},j} = \Omega_j(\omega_{\mathrm{cr}}), \quad j = 1, 2, \ldots. \end{cases} \tag{3.9}$$

In the above model, using concentrated cutting force, this critical frequency (together with the critical cutting coefficient) is always the same at any of the critical running speed values $\Omega_{\mathrm{cr},j}$, and it is just a bit greater than the (lowest) natural frequency of the machine tool. This fact often leads to a misunderstanding, when engineers identify the occurring vibration as a kind of *resonance*. Regenerative chatter is, however, a kind of *self-excited vibration*.

4. Experimental observations

(a) A case study from industry

A machine-tool vibration problem caused a bottle-neck in the manufacturing process of a workshop. A numerically controlled cutting machine was used for thread cutting using a comb-like tool of seven edges, as shown in the enlarged part of figure 4. The shaded regions explain the approximate chip formation during cutting. The thread had to be cut on the internal surface of a cylindrical workpiece. The workpiece had a length of 220 mm, while its internal diameter was about $d = 176$ mm.

Actually, the internal surface of the workpiece was slightly conical, having a diameter smaller by 3 mm at the middle cross-section than at the two ends. This had no effect on the dynamics of the cutting. However, the thread had to be cut starting from one side of the cylinder in the direction of its mid part, and it had to be repeated again from the other end. In order to achieve greater efficiency and to decrease costs, a special chock was used on the machine tool. This chock made it possible to turn over the workpiece about an axis perpendicular to the main shaft axis through the geometrical centre of the workpiece, even during the running of the main shaft (see figure 4). During this turnover, the tool was withdrawn from the cylinder, but the main shaft did not have to slow down to rest and to accelerate again; also, the workpiece had neither to be released from the chock nor to be turned over by the machinist or by a service robotic arm.

These arrangements had important dynamical consequences. The most important fact was that the bearings/shaft/chock/workpiece structural part had a low first natural frequency due to the great mass of the complicated multi-functional chock and due to the relatively low stiffness of the tubular shaft and that of the roller bearings having soft tubular rollers. The mass of the chock itself was *ca.* 340 kg, the workpiece and other oscillating parts were about another 6 kg. At the centre of the chock, the reduced stiffness of the shaft on the soft supports was about $k = 97\,\mathrm{N}\,\mathrm{\mu m}^{-1}$, according to our static measurements and simple approximate calculations.
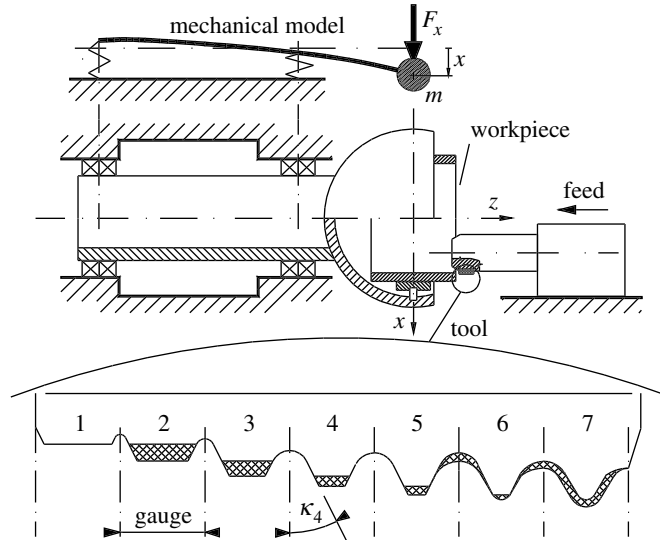
Figure 4. Thread cutting and machine-tool mechanical structure.

As the simple mechanical model in figure 4 shows, the first vibration mode in the direction normal to the main shaft had a natural frequency of

$$f_n = \frac{\omega_n}{2\pi} = \frac{1}{2\pi}\sqrt{\frac{k}{m}} = 84.1 \text{ Hz}. \tag{4.1}$$

This natural frequency was also confirmed by the results of simple impact experiments. The chock was hit by a rubber hammer, and the vibrations of the chock were detected by a piezo crystal accelerometer (while the main shaft did not rotate, of course). It was also checked, by numerical estimations, that the gyroscopic effects and the twisting torque on the shaft did not affect the natural frequency by more than 1%, neither did the increase in temperature at the bearings during rotation. Still, these may cause *ca.* 1 Hz deviation between measurement results on the same machine tool when it is out of operation and during machining. This small value can be important in the explanation of the regenerative chatter frequency deviations, where the theoretical and experimental results should coincide in a narrow frequency interval of *ca.* 6 Hz.

The impact-induced vibration signal was also useful in identifying the relative damping factor in the simplified model of figure 5. The calculation of the logarithmic decrement and its conversion to the relative damping factor gave the result of $\xi = 0.025$.

The results also confirmed that there are no other vibration modes with low natural frequencies close to the one mentioned above. Actually, this real machine was just the same, from the mechanical model viewpoint, as those which are often used in laboratory experiments, when an elastic element is fitted typically between the tool and the tool-holder (see, for example, Moon & Johnson 1998). Still, the model in figure 5 has two degrees of freedom, due to the cylindrical symmetry. According to the approach proposed by Tobias (Shi & Tobias 1984), the cutting-force variation ΔF is considered to have the same direction as the cutting force itself. This means that the oscillation of the two-DOF system can be described with the help of the
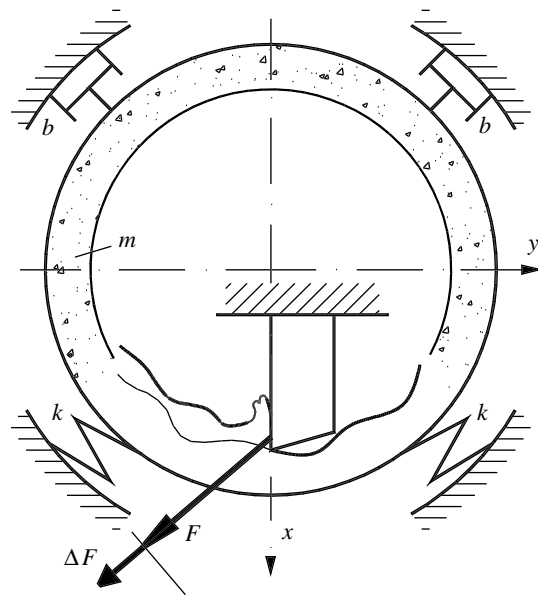
Figure 5. Mechanical model and cutting force.

single coordinate x only, which determines the variation of the chip cross-section geometry. The vibration itself will take place in the y-direction in the same manner, but this direction has no linear effect on the chip geometry, so we do not include this in the regenerative vibration model, and only the cutting-force variation in the x-direction is modelled and calculated.

(b) Cutting coefficient and overlap factor

Although the tool has seven edges (as shown in figure 4), the first does not operate according to the designed technology. The time delay between the edges remains equal to the time period of one rotation of the workpiece. This means that, in spite of the fact that the number of cutting edges is more than one, the parametric excitation effect, which occurs typically in the milling process due to the time-varying number of active tool edges (see Minis & Yanushevsky 1993), does not show up here.

There is another effect, however, which does modify the conventional linear model described in §2, and this is due to the fact that the second edge cuts the even (non-machined) surface and, thus, there is no regenerative effect there. This can be described by the use of a so-called overlap factor q in the following way.

The cutting force is estimated according to the three-quarter rule, as in (2.1). With respect to the jth tool edge, the corresponding coefficients $c_{1,j}$ in the formula

$$F_{x,j}(w_j, h_j) = c_{1,j} w_j h_j^{3/4} \tag{4.2}$$

are estimated from standard engineering tables, taking into account the ultimate stress (*ca.* 490 MPa) of the workpiece material and the spatial orientation of the cutting force relative to the x-direction (which is *ca.* $60°$ in the x, y-plane, and another $60°$ in the x, z-plane of the tool for the sides of the sixth and seventh teeth, as shown in figure 4). The calculation of the cutting-force variation in the x-direction is not an

easy task, since both the chip width w and the thickness h vary, and they do so in different ways for different groups of the edges. The total cutting-force variation in the x-direction is the sum of the variations for each tooth, and it assumes the form

$$\Delta F_x = \sum_{j=2}^{7} \Delta F_{x,j} = \sum_{j=2}^{7} \left(\frac{\partial F_{x,j}}{\partial h} \Delta h_j + \frac{\partial F_{x,j}}{\partial w} \Delta w_j \right), \qquad (4.3)$$

where the chip-thickness and chip-width variations can be expressed by the present position $x(t)$ and the past position $x(t - \tau)$ of the workpiece in the following way,

$$\left. \begin{array}{ll} \Delta h_2 = -x(t), & \\ \Delta h_j = x(t - \tau) - x(t), & j = 3, 4, 5, \\ \Delta w_j = \Delta h_j \tan \kappa_j, & j = 2, 3, 4, 5, \\ \Delta h_j = (x(t - \tau) - x(t)) \sin \kappa_j, & j = 6, 7, \\ \Delta w_j = (x(t - \tau) - x(t)) \cos \kappa_j, & j = 6, 7, \end{array} \right\} \qquad (4.4)$$

with $\kappa_j = 27°$ for teeth $j = 2, 3, 4, 5$ and $\kappa_j = 30°$ for teeth $j = 6, 7$. The actual dimensions of the chip geometry can be estimated from the tooth gauge (3.175 mm) of the comb, but it was also determined by a measurement microscope checking the worn surface of the tool edges. Note that there is no delay effect on the second tool edge (which is actually the first active tool edge). When the chip geometry variation (4.4) is substituted in the cutting-force variation formula (4.3), the cutting-force variation is expressed by the present and delayed x positions of the workpiece, but the coefficients of the two terms are not the same, due the missing delayed term at the second edge,

$$\Delta F_x = k_1 (q x(t - \tau) - x(t)). \qquad (4.5)$$

After carrying out all the detailed calculations prescribed in formulae (4.2)–(4.4), the actual value of the overlap factor becomes $q = 0.8$, and the cutting coefficient k_1 has its value at $ca.\,8.5\text{ N }\mu\text{m}^{-1}$.

The overlap factor q expresses physically how much the subsequent cuts overlap each other. Since most of the chip material is removed by the second tooth of the tool, the actual value of 0.8 is quite small relative to the usual value of 1 in standard regenerative vibrations, and it does have an effect of $ca.\,10$–15% on the stability limits. The value of the cutting coefficient k_1 is a less reliable quantity, since the coefficients $c_{1,j}$ in the cutting-force formulae (4.2) come from experimental data carried out during stationary cutting to provide simple-to-use formulae for technology design.

Finally, the actual length of the chip and tool face contact length in x-direction was also measured, again, by checking the wear on the cutting surface under a microscope. This length, denoted by l in §2 (and in figure 1), was always less than 0.6 mm. The comparison of the short and long time delay in this case shows that

$$\frac{\sigma}{\tau} = \frac{l/v}{d\pi/v} = \frac{l}{d\pi} = \frac{0.6}{176\pi} \approx 0.001.$$

This means that the short regenerative effect is really negligible in the middle range ($\Omega = 100$–400 RPM) of cutting speeds and the concentrated cutting-force approach can be used, as explained in §2 during the comparison of the mathematical models (2.8) and (2.10).
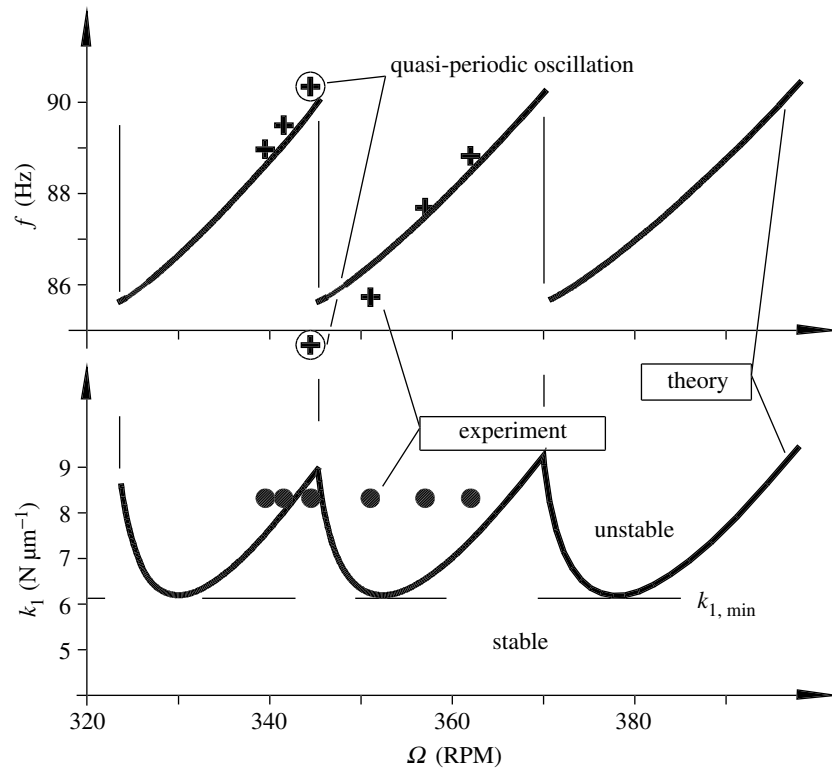
Figure 6. Theoretical and experimental stability chart.

(*c*) *Linear stability—theory and measurements*

The above-explained equation of motion assumes the form

$$\ddot{x}(t) + 2\xi\omega_{\mathrm{n}}\dot{x}(t) + \left(\omega_{\mathrm{n}}^2 + \frac{k_1}{m}\right)x(t) - \frac{k_1}{m}qx(t-\tau) = 0, \tag{4.6}$$

which would be identical to (2.10) if the overlap factor q were 1. The stability chart of this linear model can be constructed with the help of the same closed-form calculations (3.5)–(3.8) as described by Stépán (1989), but the results are affected somewhat by the overlap factor. The resulting stability chart in figure 6 shows the theoretically calculated stability limit, where the circles refer to the parameters of the measurement points.

Practically, the parameters of all the working points fall in the unstable domain, except that of the third at $\Omega = 344$ RPM. Vibrations with different frequencies occurred in all cases, even in the third which is supposed to be within the linear stability limit. The measured and calculated vibration frequencies fit together quite well.

Clearly, greater domains of stability could be found at higher cutting speeds with the same value of the cutting coefficient. However, the power of the given machine tool gave a limitation to increasing the speed above *ca.* 370 RPM, that is, the safer regions of stable cutting were beyond reach.

(d) Nonlinear phenomena in the measured signals

As explained in § 2, it is usually the cutting-force nonlinearity which has the most important effect on the nonlinear behaviour. In the experimentally studied machine tool there was no structural nonlinearity which could have been suspected to have a comparable effect to that of the cutting force. The nonlinear cutting-force characteristic in figure 2 has two important parts. The non-symmetric characteristic of the function around the theoretical chip thickness h_0 has a central role in why the analytical calculation and approximation of a possible unstable periodic motion is so complicated (see Stépán & Kalmár-Nagy 1997). This non-symmetry means that the Taylor series of the function will also contain even- (i.e. second-, fourth-, etc.) degree terms. The Taylor expansion of the Taylor formula about the theoretical chip thickness h_0 corresponds to the expansion of the cutting-force variation ΔF_x about zero with respect to the chip-thickness variation Δh,

$$\Delta F_x(\Delta h) = \sum_{j=1}^{3} \frac{1}{j!} k_j (\Delta h)^j. \tag{4.7}$$

Following from the differentiation in the Taylor formula, the first three coefficients of the series depend on the theoretical chip thickness h_0 and the (constant) chip width w as follows:

$$k_1 = \tfrac{3}{4} c_1 w h_0^{-1/4}, \qquad k_2 = -\frac{1}{4} \frac{k_1}{h_0}, \qquad k_3 = \frac{5}{16} \frac{k_1}{h_0^2}. \tag{4.8}$$

The first parameter k_1 has already been defined as the cutting coefficient in (2.2).

The other important part of the characteristic is at zero chip thickness. Since there is no negative chip thickness, the characteristic has a kink at zero; it is not differentiable there. The zero value of the cutting force for negative h values refers to the case where the tool actually leaves the material of the workpiece. This nonlinearity becomes important for large oscillations, and will be responsible for the global behaviour of the tool during the nonlinear regenerative chatter (see also Batzer *et al.* (1999) for the case of drilling).

Note also that an inflection may show up in the cutting-force characteristic at large chip thicknesses of h_{inf}, as shown by the measurements of Shi & Tobias (1984), for example. This value may be of theoretical importance only, but the bifurcation calculations can be carried out much more easily at this point, since the secondary cutting coefficient k_2 becomes zero in this case. These calculations show that the subcritical nature of the Hopf bifurcation, i.e. the possible existence of an unstable limit cycle, remains unchanged.

The photograph of the machined workpiece in figure 7 shows the so-called 'sun-flower spirals' on its surface, which are so typical for regenerative chatter. This surface is analysed for a workpiece manufactured at the cutting speed $\Omega = 344$ RPM. The signal, taken by an inductive displacement detector, is presented in figure 8. Each line of signal represents one rotation of the workpiece, that is, it has the time-length just equal to the time delay $\tau = 60/\Omega = 0.175$ s. In spite of the fact that the actual technological parameters fall in the stable domain (as shown in the stability chart), the workpiece starts increasing oscillations, due to some perturbation which pushed the system 'outside' the inset (or basin) of one of the unstable limit cycles. The
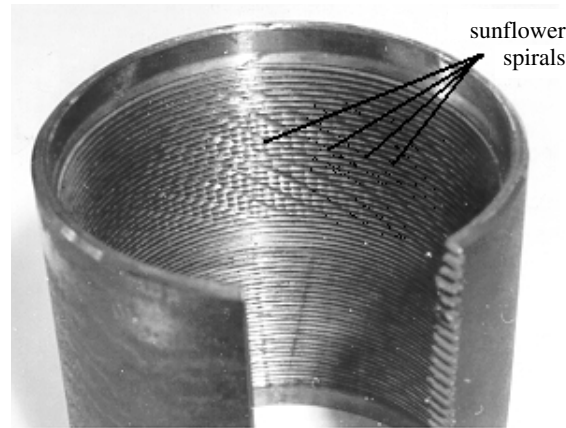
Figure 7. Workpiece surface after violent vibrations during thread cutting.

existence of these limit cycles was predicted in several research reports (see Shi & Tobias 1984; Nayfeh *et al.* 1997). In the paper of Stépán & Kalmár-Nagy (1997), the unstable limit cycle is estimated to exist within an 8% range below the critical cutting coefficient, which is the case in the experiment at 344 RPM, as shown in figure 6. Since the actual parameter point is close to a peak between two lobes in the stability chart, two unstable periodic motions may be present at the same time, with two slightly different frequencies, as shown by the frequency diagram above the stability chart of figure 6. The combination of the two periodic motions (independent of their stability) may easily result in quasi-periodic motions as well. The existence of possible parameter domains where stable or unstable quasi-periodic vibrations may occur with two nearby frequencies in them can also be studied by the methods of bifurcation theory.

The corresponding codimension-2 bifurcation diagram in figure 9 shows the most likely scenario at one of the critical peak points of the stability chart: in one of the parameter sectors, the trajectories get involved in a quasi-periodic oscillation (topologically, in a torus) after leaving the unstable limit cycle 'outwards'. However, the torus itself is again unstable (saddle-like). The small two-dimensional phase plots represent the two radii of the polar coordinates of the four-dimensional centre manifold belonging to the critical parameter values, where two pairs of complex conjugate characteristic roots appear in the imaginary axis of the complex plane with two different but nearby imaginary parts. In these phase plots, the two rotations are not shown. Consequently, the trivial fix point 0 represents the (asymptotically stable) stationary cutting, the non-trivial fix points in the axes refer to (unstable) limit cycles, while the fix point in the positive quadrant refers to an (again, unstable) torus.

For the time being, this bifurcation diagram can be calculated for the above-mentioned case of the inflection point of the cutting-force characteristic only, since the analytical calculations are too complicated, even with the use of computer algebra. A similarly detailed closed-form calculation is presented for a time-delay system in robotics, with a topologically conjugate result showing two stable limit cycles and a saddle-like unstable torus in between, for a parameter sector on the opposite (unstable) side of the chart (see Stépán & Haller 1995).
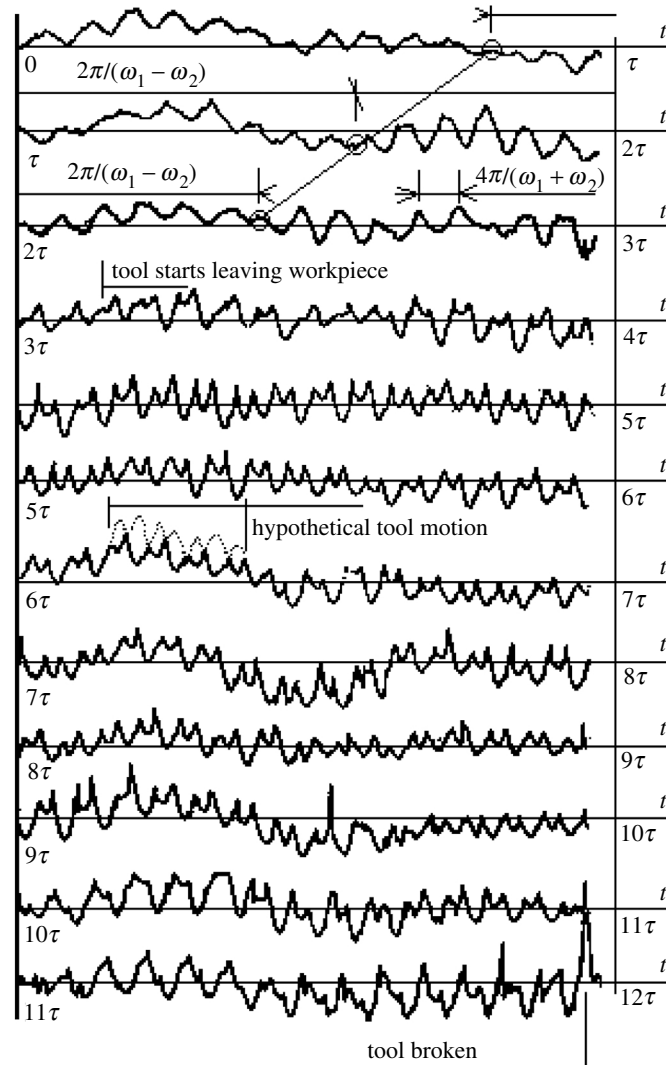
Figure 8. Measured surface of the workpiece.

Note that the algebraic calculations are so complex that they may lose their credibility in these cases; the simulation results may also be questioned due to the infinite-dimensional phase-space structure, and the unstable periodic and quasi-periodic motions can hardly be identified by either simulation or measurements. Still, a simple analysis of the surface signal in the first part of figure 8 (and others similar) supports the above-described mechanism of the evolution of the nonlinear oscillation. Two vibration frequencies can be identified from the vibration signal simply by numbering two subsequent periods of the beating effect marked in figure 8 within the first 3–4 periods of rotation in the signal. Since *ca.* 15.3 periods of oscillations can be counted in one time period τ, and the marked beating effect takes *ca.* 2×12.5 oscillations, the sum and difference of the two component vibration
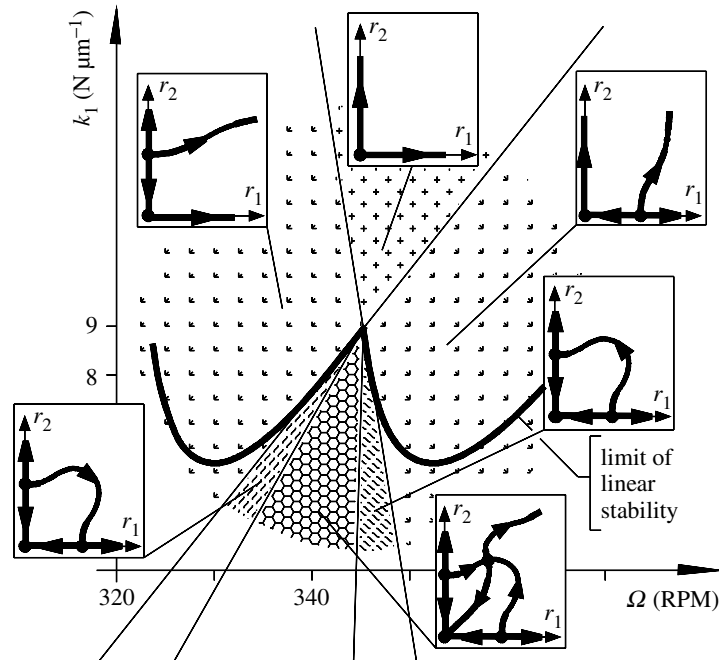
Figure 9. Codimension-2 bifurcation diagram.

frequencies are calculated as follows,

$$\tfrac{1}{2}(\omega_1 + \omega_2) = \frac{15.3}{\tau} = 88.0\ \text{Hz}, \qquad \tfrac{1}{2}(\omega_1 - \omega_2) = \frac{15.3}{2 \times 12.5}\frac{1}{\tau} = 3.5\ \text{Hz}, \qquad (4.9)$$

which yields

$$\omega_1 = 91.5\ \text{Hz}, \qquad \omega_2 = 84.5\ \text{Hz} \qquad (4.10)$$

These are just the frequencies which are plotted in the stability chart of figure 6 at the running speed 344 RPM.

(e) *Chaos and/or transient chaos*

Based on the above experimental evidence and the accompanying theoretical calculations, let us discuss the possible motion of the system in that region of the technological parameters where the stationary cutting is actually asymptotically stable, and unstable periodic and quasi-periodic motions exist around it, as shown in figure 10. The heteroclinic orbits connecting the (unstable) periodic and quasi-periodic solutions form a three-dimensional set in the four-dimensional subspace (originated in a centre manifold) of the infinite-dimensional phase space of the cutting (i.e. delayed) dynamics. This three-dimensional set shows up as a line in the polar coordinate representation of the four-dimensional subspace, since the two rotations are not presented. This three-dimensional set borders the domain of attraction of the stable stationary cutting. When a certain motion starts 'outside' this set, as shown in figure 10, the vibrations start increasing, in spite of the fact that the cutting is linearly stable. First, the trajectory may approach the torus, which means that the increasing vibrations show a quasi-periodic nature for a certain time period, and the machinist
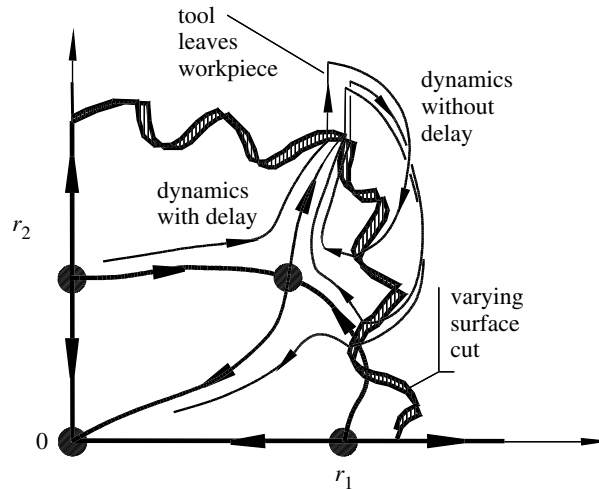
Figure 10. Switches between regenerative dynamics and damped oscillations.

may even sometimes expect their disappearance when the beating effect is just in the decreasing amplitude range. But this is not so. The vibrations will continue to increase with greater and greater wave amplitudes as the trajectory starts leaving the (saddle-like unstable) torus 'outwards'.

At this point, another important nonlinearity comes into the picture: the cutting force becomes zero for negative chip thickness (see figure 2), that is, the tool leaves the workpiece material and the regenerative effect (together with the time delay) is switched off, suddenly. Physically, this process is represented by that part of the manufactured surface of the workpiece shown in figure 8, where the hypothetical path of the tool is also presented by dotted lines above the fractal-like surface. These vibrations continue in a violent way until, in the end of the process, the teeth numbered 6 and 7 (see figure 4) are broken and actually left in the workpiece material. In the schematic phase-space topology of figure 10, the separation of the tool and the workpiece means that the trajectory jumps from the delayed infinite-dimensional dynamics to the two-dimensional dynamics of a simple damped oscillator at the cutting surface (which, actually, also moves; 'rotates'). Clearly, the damped-oscillator dynamics will push the trajectory back into the delayed dynamics, describing the physical process as the tool hits the workpiece material soon after leaving it. Then the above-described switches between the two dynamics may be repeated several times, resulting in a complicated and irregular behaviour.

It is likely that the resulting vibration is chaotic, and the surface of the workpiece, as a trace of this motion, becomes a fractal, as already proposed by Moon & Johnson (1998). It is also a possible scenario that the tool may actually arrive back at the regenerative dynamics 'inside' the border of the basin of attraction of the stationary cutting, as shown in the last part of the sample hypothetical trajectory in figure 10. This means that after a periodic, then quasi-periodic, then chaotic, motion, the tool can still jump back to the stable stationary cutting. However, the time-length of this transient chaotic behaviour (if it occurs at all) varies stochastically, and it may be so long that the whole cutting process is over in the meantime. This explains why this phenomenon is experienced so rarely.

5. Summary

The simplest detection of the machined surface in the case of thread cutting led to a description of the complex vibration development on machine tools, and the mechanism of this development was implemented in the infinite-dimensional phase space with a finite-dimensional topological picture. The experienced temporary periodic and quasi-periodic motions refer to unstable limit cycles and tori in the phase space. Also, chaotic and/or transient chaotic oscillations can be expected in the final stage of the vibration development.

From a practical viewpoint, the moral of this story is two-fold. The linear stability theory (which is already quite complicated to implement due to parameter uncertainties and the infinite-dimensional nature of the dynamics) does have a limited practical meaning, since the presence of unstable periodic and/or quasi-periodic motions make the stationary cutting sensitive to perturbations kicking the system out of the basin of attraction. The estimations based on Hopf bifurcation calculations and experiments show that the global stability of stationary cutting can be expected to be 8–10% below the linear stability limit only. On the other hand, when the vibrations outside the basin of the stationary cutting are initiated by some perturbations, the temporary decrease in the vibrations follows a beating effect only, and the vibrations will return, and increase further. Still, when the motion already looks violent and irregular, the vibrations can disappear if the tool jumps back to the material at a 'lucky' point of the infinite-dimensional phase space, which leads the system back to the sensitive, but linearly stable, stationary cutting.

References

Balachandran, B. & Zhao, M. X. 2000 A mechanics based model for study of dynamics of milling. *Meccanica* **35**, 89–109.

Batzer, S. A., Gouskov, A. M. & Voronov, S. A. 1999 Modeling the vibratory drilling process. In *Proc. 17th ASME Biennial Conf. on Vibration and Noise, Las Vegas, NV*, Paper no. DETC99/VIB-8024, pp. 1–8.

Bayly, P. V., Young, K. A. & Halley, J. E. 1999 Tool oscillation and the formation of lobed holes in a quasi-static model of reaming. In *Proc. 17th ASME Biennial Conf. on Vibration and Noise, Las Vegas, NV*, Paper no. DETC99/VIB-8061, pp. 1–11.

Davies, M. A. 1998 Dynamic problems in hard turning, milling and grinding. In *Dynamics and chaos in manufacturing processes* (ed. F. C. Moon), pp. 57–91. Wiley.

Davies, M. A. & Burns, T. J. 1999 The dynamics of chip formation in machining. In *New applications of nonlinear and chaotic dynamics in mechanics* (ed. F. C. Moon), pp. 183–192. Dordrecht: Kluwer Academic.

Davies, M. A., Burns, T. J. & Evans, C. J. 1997 On the dynamics of chip formation in machining hard metals. *Ann. CIRP* **46**, 25–30.

Grabec, I. 1988 Chaotic dynamics of the cutting process. *Int. J. Machine Tools Manufacturing* **28**, 19–32.

Halley, J. E., Helvey, A., M., Smith, K. S. & Winfough, W. R. 1999 The impact of high speed machining technology on the design and fabrication of aerospace components. In *Proc. 17th ASME Biennial Conf. on Vibration and Noise, Las Vegas, NV*, Paper no. DETC99/VIB-8057, pp. 1–5.

Hanna, A. & Tobias, S. A. 1974 A theory of nonlinear regenerative chatter. *ASME J. Engng Industry* **96**, 247–255.

Kalmár-Nagy, T., Pratt, J., Davies, M. A. & Kennedy, M. D. 1999 Experimental and analytical investigation of the subcritical instability in metal cutting. In *Proc. 17th ASME Biennial Conf. on Vibration and Noise, Las Vegas, NV*, Paper no. DETC99/VIB-8060, pp. 1–9.

Kuang, Y. 1993 *Delay differential equations.* Academic.

Marusich, T. D. & Ortiz, M. 1995 Modeling and simulation of high-speed machining. *Num. Methods Engng* **38**, 3675–3694.

Minis, I. & Berger, B. S. 1998 Modeling, analysis, and characterization of machining dynamics. In *Nonlinear dynamics of material processing and manufacturing* (ed. F. C. Moon), pp. 125–164. Wiley.

Minis, I. & Yanushevsky, R. 1993 A new theoretical approach for the prediction of machine tool chatter in milling. *J. Engng Industry* **115**, 1–8.

Moon, F. C. & Johnson, M. A. 1998 Nonlinear dynamics and chaos in manufacturing processes. In *Nonlinear dynamics of material processing and manufacturing* (ed. F. C. Moon), pp. 3–32. Wiley.

Nayfeh, A. H., Chin, C.-M. & Pratt, J. 1997 Applications of perturbation methods to tool chatter dynamics. In *Nonlinear dynamics of material processing and manufacturing* (ed. F. C. Moon), pp. 193–213. Wiley.

Shi, H. M. & Tobias, S. A. 1984 Theory of finite amplitude machine tool instability. *Int. J. Machine Tool Design Res.* **24**, 45–69.

Stépán, G. 1989 *Retarded dynamical systems.* New York: Longman.

Stépán, G. 1998 Delay-differential equation models for machine tool chatter. In *Dynamics and chaos in manufacturing processes* (ed. F. C. Moon), pp. 165–192. Wiley.

Stépán, G. 1999 Delay, nonlinear oscillations and shimmying wheels. In *New applications of nonlinear and chaotic dynamics in mechanics* (ed. F. C. Moon), pp. 373–386. Dordrecht: Kluwer Academic.

Stépán, G. & Haller, G. 1995 Quasiperiodic oscillations in robot dyanmics. *Nonlinear Dynamics* **8**, 513–528.

Stépán, G. & Kalmár-Nagy, T. 1997 Nonlinear regenerative machine tool vibrations. In *Proc. ASME Design Engineering Technical Conf. on Vibration and Noise, Sacramento, CA*, Paper no. DETC97/VIB-4021, pp. 1–11.

Tlusty, J. 1978 Analysis of the state of research in cutting dynamics. *Ann. CIRP* **27**, 583–589.

Tlusty, J. & Spacek, L. 1954 *Self-excited vibrations on machine tools.* Prague: Nakl CSAV. (In Czech.)

Tobias, S. A. 1965 *Machine tool vibrations.* London: Blackie.

Usui, E., Shirakashi, T. & Kitagawag, T. 1978 Analytical prediction of three dimensional cutting process. *J. Engng Industry* **100**, 236–243.

Wang, Z. H. & Hu, H. Y. 1999 Robust stability test for dynamic systems with short delays by using Padé approximation. *Nonlinear Dynamics* **18**, 275–287.

Wiercigroch, M. 1997 Chaotic vibration of a simple model of the machine tool cutting process system. *ASME J. Vib. Acoust.* **119**, 468–475.